Four-year observations of T Tauri with adaptive optics

C. Roddier[1], F. Roddier[1], J. E. Graves[1], M. J. Northcott[1],
L. Close[1], J. Surace[1], and J. P. Veran[2].

[1]*Institute for Astronomy, University of Hawaii, USA*

[2]*Dominion Astrophysical Observatory, Canada*

Abstract

We report here on a series of adaptive optics observations of T Tauri made from Dec. 1993 to Nov. 1997. Observations show an arc-like structure extending toward north and north-west. On the south side a bright tail-like structure extends radially in the south-west direction. Both structures seem to be produced by dust scattering. Close to T Tauri, the south structure forms bright clumps near a radio source called T Tau R. From one year to another, the clumps appear to be moving toward T Tauri. The infrared companion is detected for the first time in the J band. Its brightness peaked again in 1996, although the maximum was less pronounced than in 1990. It is found to be resolved with a radius of 54 milliarcsec (7.6 AU at 140 pc). Surprisingly, its orbital speed is found to exceed the escape velocity. This leads to the conjecture that T Tauri is the result of a collision between a young star and a protostar, possibly explaining the peculiar molecular hydrogen emission found in this object. The protostar envelope would have been torn apart forming Burnham's nebula and leaving the protostar naked, that is visible in the near IR .

1. Introduction

Although considered as a prototype for low-mass pre-main-sequence stars, T Tauri has unique characteristics. It is surrounded with a reflection nebula (Burnham's nebula) extending several arcseconds south (Herbig 1950). At 2.12 μm, it shows an unusual extended molecular hydrogen emission discovered by Beckwith *et al.* 1978 and mapped by van Langevelde *et al.* 1994 (see also Quirrenbach, A. and Zinnecker, H 1997). Spectral line ratios indicate shock heating is the main excitation mechanism (Herbst *et al*. 1996). It has an infrared companion T Tau South discovered by Dick *et al*. (1982), the nature of which is still debated. The companion has many properties generally attributed to protostars (Hanson *et al.* 1983, Bertout 1983, Maihara and Kataza 1991), but its spectral energy distribution shows a lack of cold dust normally expected around these objects (Ghez *et al.* 1991). At visible wavelength, coronagraphic images (Nakajima and Golimowski 1995) of the close environment of T Tauri show a reflection nebulosity in the form of an arc north of T Tauri and extending toward the north-west. A similar arc is also seen in images taken in the visible with the Hubble Space Telescope (HST), together with a bright tail pointing toward the south-west (Fig. 1a). This structure has been interpreted as produced by a limb brightened outflow cavity (Stapelfeldt *et al.* 1998). However, the model implies that the cavity is viewed about 45˚ from the outflow axis, which contradicts observations by Herbst *et al.* (1986) that T Tauri is seen nearly pole-on. Also the position angle the axis (PA = 300˚) does not coincide with that of known outflows (Böhm and Solf 1994).

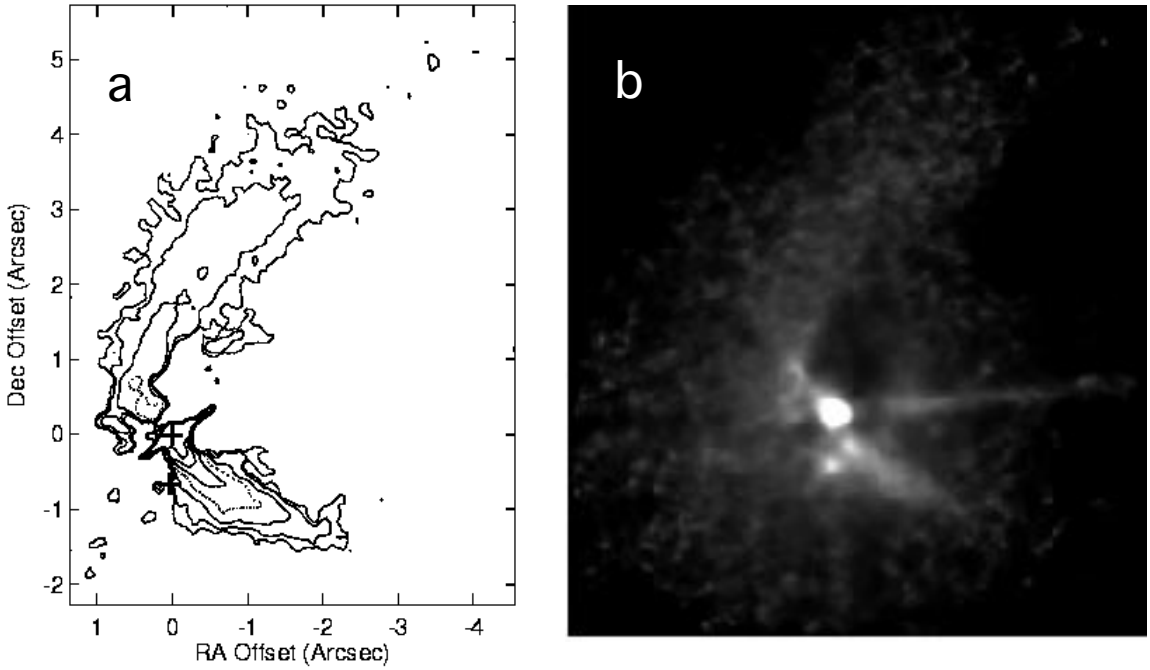

Fig. 1. High angular resolution images of T Tauri: (a) HST 0.55 μm brightness map (Stapelfeldt *et al.* 1998); (b) Deconvolved J-band AO image. Both images were obtained in 1994 and are displayed here at the same scale. North is up and east is left. On the HST image, the location of the unseen IR companion is marked with a cross. On the AO J-band image, it is detected here for the first time. Both images are affected by artifacts due to the telescopes spider arms (bright 45˚ streak on the HST image; bright nearly horizontal streak on the AO image).

2. Morphology

We present here the results of a series of observations of T Tauri made in the near infrared with adaptive optics (AO). Observations were made at the Canada-France-Hawaii Telescope (CFHT) in Dec. 1993, Dec. 1994, and October 1996 with the University of Hawaii (UH) 13-actuator AO system, and in Nov. 1997 with the new UH 36-actuator AO system called Hokupa'a. Figure 1 shows a comparison between a visible (0.55 μm) HST image taken in March 1994 (Stapelfeldt *et al.* 1998) and a J-band (1.2 μm) AO image taken in Dec. 1994. North of T Tauri, the arc structure is clearly seen on both images. The tail extending toward the south west, which is very bright on the HST image, appears less bright on the J-band image. AO images also taken in Dec. 1994 in the I band (0.85 μm) and in the H band (1.65 μm) show a continuous decrease of the tail brightness from the visible to the infrared, indicative of light scattered by small particles. Fig. 1b shows that close to the main star called hereafter T Tau North the tail starts as a bright point source, possibly a clump of material. Observations described in Section 3 show the clump evolution with time. The point source seen almost exactly south of T Tau North, becomes much brighter at longer wavelengths and has been identified with T Tau South. This is the first detection of T Tau South in the J band (Roddier *et al.* 1995). It should be noted that the AO image is deeper than the HST image. At low light levels, it shows a nearly circular distribution of scattered light around T Tau North which is consistent with the coronagraphic observations of Nakajima and Golimowski (1995) and may come from a disk seen nearly pole-on. We also reproduce here an H-band image of T Tauri obtained in November 1997 with the new 36-actuator Hokupa"a system (Fig. 2). It reveals faint annular structures also seen on other images but with less resolution. Similar but larger structures appear further away and were interpreted as "wind inflated bubbles" by Herbst et al. (1997).

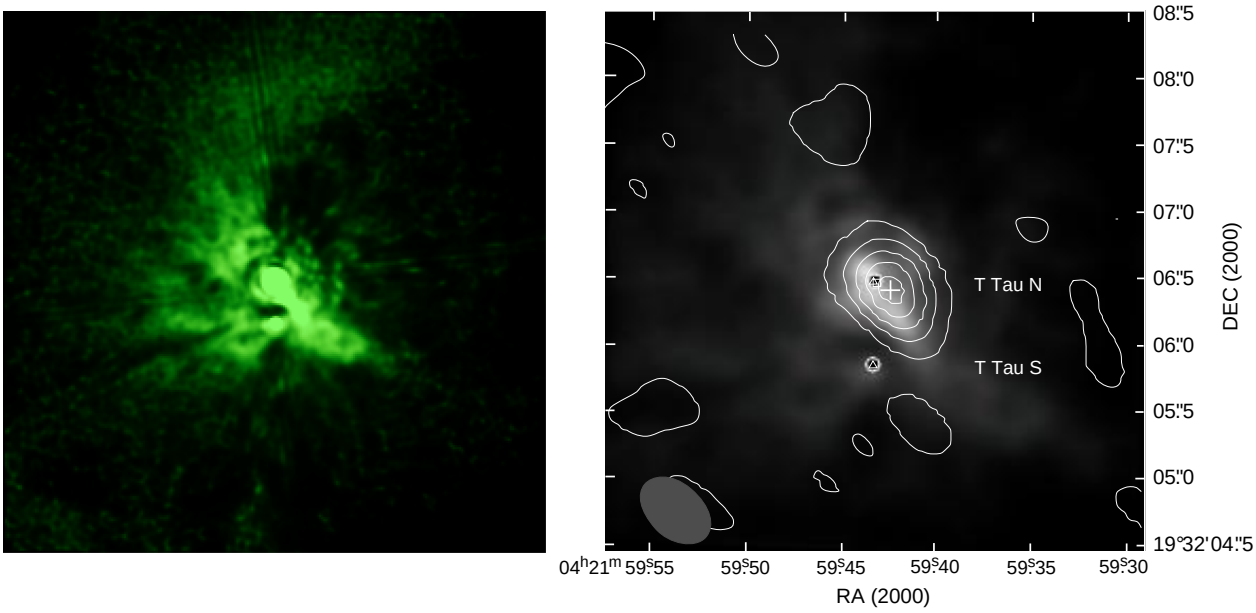

Fig. 2. Data recorded in the H band in Nov. 1997. *Left*: Deconvolved T Tauri image (same orientation as in Fig. 1). Apart from the remnants of diffraction rings around T Tauri, most of the structures seen here are real. Note the two annular structures in the southwest tail. Similar rings appear on the north side of T Tau North and on the south east side of T Tau South. Larger but much fainter rings or cavities can also be seen in the lower left side of the image. They are also seen in the images of Herbst *et al.* (1997) and were interpreted as wind-inflated bubbles. *Right*: Enlarged (x 2) P-Lucy deconvolved image. The contribution of the two stars has been removed leaving only the close stellar environment. The location of the stars is marked with black dots. Note the accumulation of material around T Tau North. Superimposed to this image, are reproduced the contour lines of the 3-mm continuum emission mapped by Akeson et al. (1998). Both observations appear to be in close agreement.

3. Time evolution

Figure 3 shows a mosaic of images deconvolved with the P-Lucy algorithm. In these images, the contribution of the stars has been removed leaving only the circumstellar environment. The location of the two stars is marked with black dots. There are certainly many artifacts in these images due to errors in the estimation of the point spread function (PSF). However, bright clumps systematically appear on the south-west side of T Tau North and must be real. No such clumps appear on images of other stars which have been processed in the same way. These clumps could be related to the 2-cm radio emission observed in the same region with the VLA by Schwartz *et al.* 1986. They are also close to the 6-cm radio source T Tau R identified by Ray *et al*. (1997) with MERLIN. On Fig. 3 they appear to be moving toward T Tau North. The direction of motion coincides with that of the Hα emission detected by Devaney *et al.* (1995) using speckle interferometry. Perhaps we see here material falling onto the star and being accreted by it. The motion speed is surprisingly high and seems to exceed the free fall velocity. The middle image on the bottom of Fig. 3 is shown expanded on the right side of Fig. 2, together with the contour lines of the 3-mm emission observed in March 1997 by Akeson *et al.* (1998). There is a clear agreement between these two observations. The millimetric observations were interpreted as arising from a circumstellar disk around T Tau North. If our interpretation is correct, we see here mostly material rapidly falling onto the star.

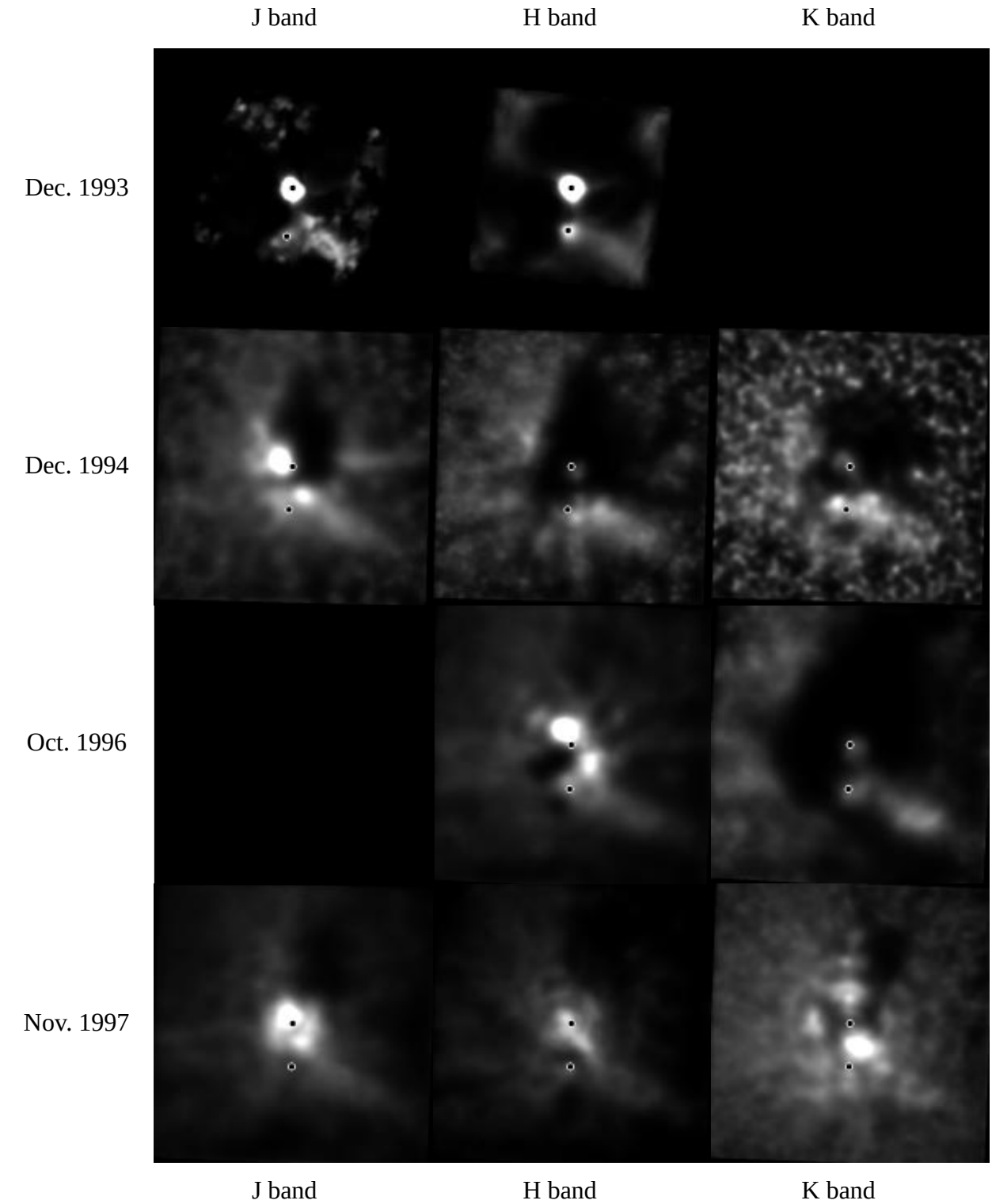

Fig. 3. The P-Lucy algorithm has been used to deconvolve these images. Contributions of both T Tau North and T Tau South have been removed leaving only the contribution of the close circumstellar environment. The location of the stars is marked with a black dots. Note the systematic presence of material on the south west side of T Tau North, apparently moving toward it.

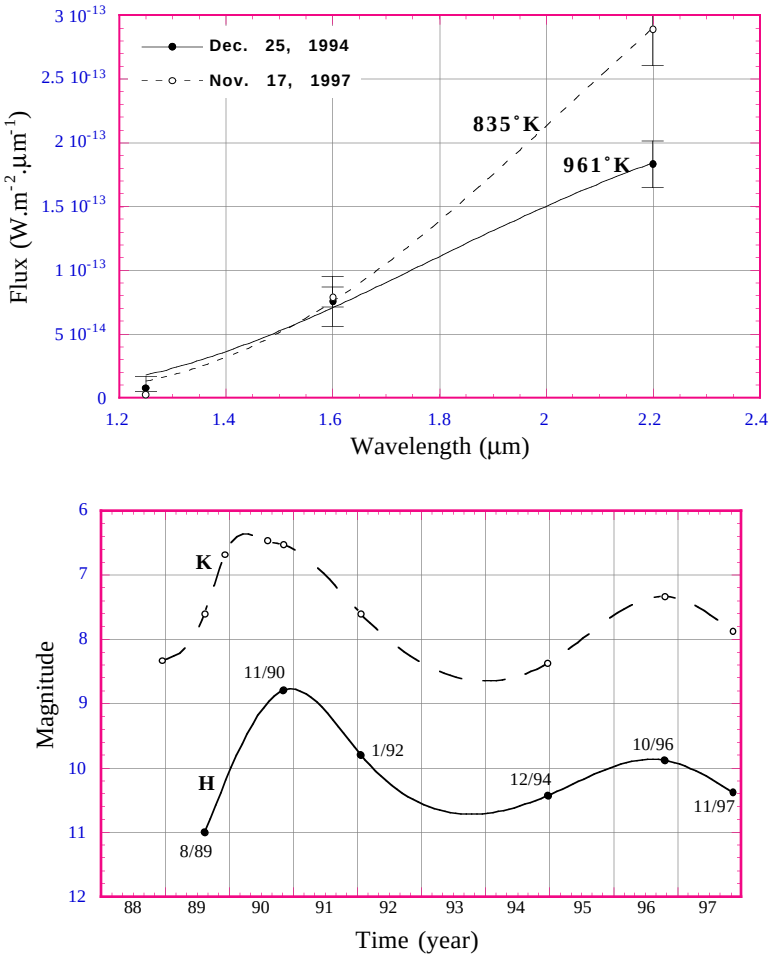

Fig. 4. *Top*: Spectral energy distribution of T Tau South estimated from two different sets of observations (open and full circles with error bars), showing evidence for time variations. A least-square fit with blackbody curves (full and dashed lines) gives the source color temperature. *Bottom*: Fluctuations of the H and K magnitudes of T Tau South as a function of time. Data before 1993 are from Kobayashi *et al*. (1991).

4. Photometry

We have compared the brightness of T Tau South to that of T Tau North and estimated their flux ratios. Photometric measurements made since 1989 on resolved images have shown no significant variations of the brightness of T Tau North (Ghez *et al.* 1991, Kobayashi *et al*. 1994). We have therefore entirely attributed the observed time variations to fluctuations in the brightness of T Tau South. The following results depend on this assumption. For the magnitude of T Tau North, we used standard values taken in the literature $m_J = 7.2$, $m_H = 6.3$, and $m_K = 5.6$. The H and K magnitudes are the most recent values from Kobayashi *et al*. (1994). Using these values, we have estimated the spectral energy distribution of T Tau South for two different data sets. The results are plotted in Fig. 4 together with a least square fit with black body curves. It shows that the color temperature of the companion has varied from 835˚ in Dec. 1994 to 961˚ in Nov. 1997. Fig. 5 shows the variation of the companion H and K magnitudes as a function of time. Data before 1993 are from the compilation of Kobayashi *et al*. (1994). Clearly, the companion brightness peaked again in 1996, although the maximum was less pronounced than in 1990.

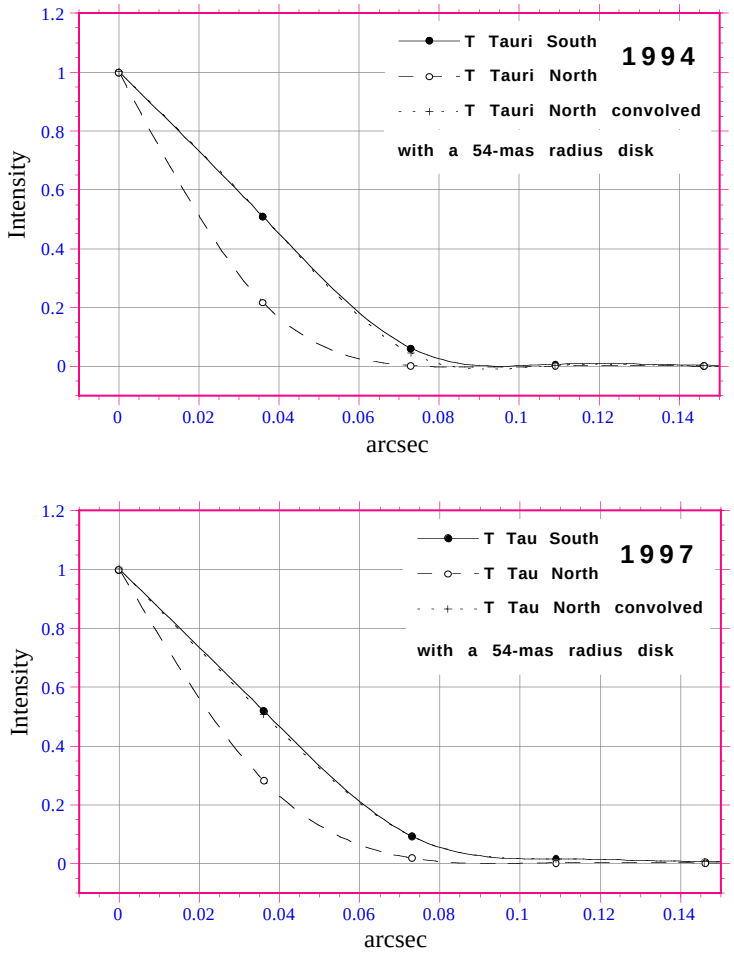

Fig. 5. Comparison between the intensity profiles of T Tau North (open circles) and T Tau South (full circles). The profiles are circular averages obtained from deconvolved H-band images. For both data set (*Top*: 1994; *Bottom*: 1997) the profile of T Tau South can be fitted by convolving that of T Tau North with a uniform 54-mas disk.

5. Astrometry

A comparison between the intensity profile of T Tau North and that of T Tau South (see Fig. 5) shows that T Tau South is angularly resolved, as suggested by the observations of Maihara and Kataza (1991). To estimate the radius of T Tau South we have convolved the image of T Tau North with a uniformly illuminated disk and compared the result to the image of T Tau South. The radius of the disk was adjusted until a good fit was obtained. This was done on both H band and K band data taken in 1994, 1996 and 1997. In all cases we found the best fit was obtained with a disk radius of 54 ± 2 milliarcsecond. Figure 5 shows the result of the fit for two sets of data (1994 and 1997) obtained in the H band.

We have also measured the offset position of T Tau South compared to T Tau North. On two occasions (Dec. 1994 and Nov. 1997) the plate scale and orientation was calibrated using GG Tau A and B as a reference. These two objects are about 10” apart and are known to be physically bound. Their relative positions can be found in Leinert *et al*. (1993). Since the mass of GG Tau is known from the motion of the close companion GG Tau a (Roddier et al. 1996), one can set an upper limit to the

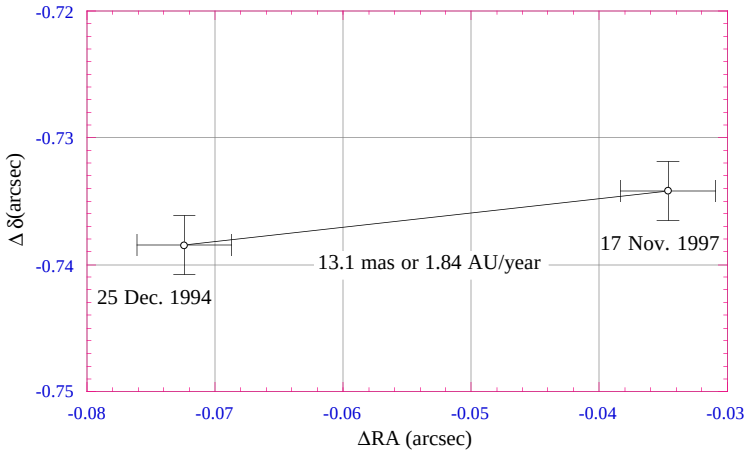

Fig. 6. Offset position of T Tau South compared to T Tau North. The absolute uncertainty on the offset values is ± 0.025" in RA and ± 0.015" in δ . However, the relative uncertainty on the two offset positions is much smaller as indicated by the error bars.

apparent motion of GG Tau B with respect to GG Tau A by stating that the observed velocity v should not exceed the escape velocity. This gives an upper limit for the apparent motion of GG Tau B relative to GG Tau A,

$$v \leq \sqrt{\frac{2GM}{a}}\,, \tag{1}$$

where M is the mass of the system and a the apparent distance of the two components. With M = 1.4 M_o and a = 1440 AU, one has $v \leq 0.28$ AU/year, *i.e.* 2 milliarcsecond/year or 6 milliarcsecond over 3 years. For a separation angle of 0.73" the error reduces to 0.4 milliarcsecond that is 10 times smaller than the estimated error on our position measurements (error bars on Fig. 6). Figure 6 shows the resulting offset positions for the indicated dates. The absolute error on these offset values (indicated in the figure caption), is much larger than the error bars, and is set by the accuracy of the measurements made by Leinert *et al.*(1993) and indicated in their paper. The difference between the two offset positions gives an apparent orbital velocity of 13.1 ± 2.6 milliarcsecond/year or, at a distance of 140 pc, 1.84 ± 0.36 AU/year (8.76 ± 1.71 km/s). This result differs somewhat from that of Ghez *et al*. (1995) who find 1.11 ± 0.11 AU/year (5.3 ± 0.52 km/s). However, we believe adaptive optics measurements are less prone to systematic errors than speckle measurements.

6. Interpretation

Assuming that T Tau North and T Tau South are gravitationally bound, our above derived velocity gives a minimum mass for the T Tauri system,

$$M = \frac{v^2 a}{2G}\,, \tag{2}$$

where v is the observed apparent orbital velocity, and a is the observed projected distance between the two components. Taking v = 1.84 AU/year and a = 103 AU gives M = 4.42 M_o. This is significantly higher than the current estimate $M \approx 3\ M_o$ for the total mass of the T Tauri system (Weintraub *et al.* 1989). If we take our lower bound v = 1.48 AU/year, we obtain a minimum mass M = 2.86 M_o

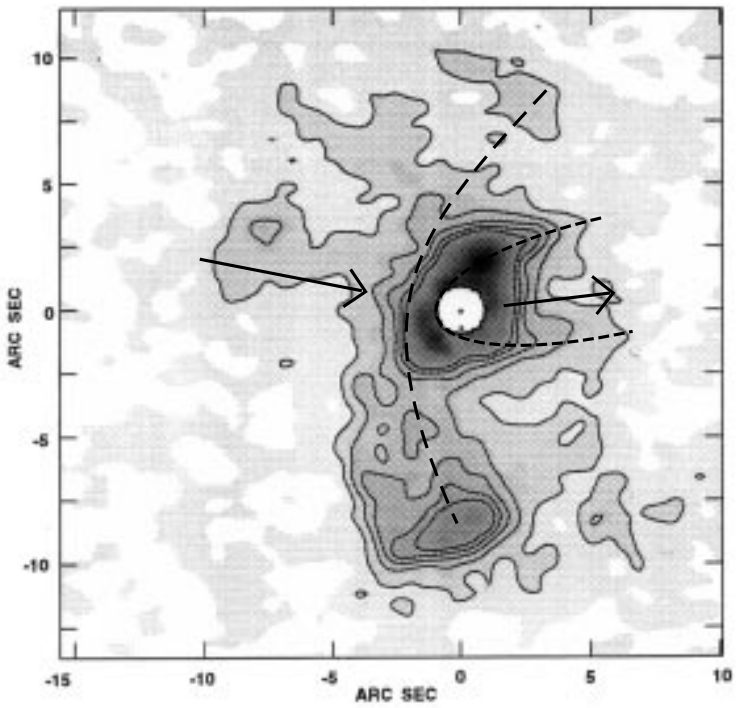

Fig. 7. Map of the H2 emission from van Langevelde *et al.* (1994). Added to the map are dashed lines showing C shape features possibly produced by bow shocks, and arrows showing the direction of the companion motion.

which becomes acceptable but implies that the companion has a highly eccentric orbit. In the following, we discuss the possibility that T Tau North and T Tau South may not be gravitationally bound.

There is evidence that both stars are physically associated. On some radio maps, they are seen linked with a bridge of material (Schwartz *et al*. 1986). However, if they are not gravitationally bound, they may not be coeval. An interesting possibility is that we are seeing here a collision between a protostar and a young star. Although a possibly rare event, it may –as we shall see– explain many of the T Tauri unusual characteristics:

1) Protostars are usually hidden inside a large highly opaque envelope of material still in a condensing stage and often referred to as a "cocoon". If such a cocoon happens to hit an already condensed object, it will break apart. That would explain Burnham's nebula. It should be noted that the companion is passing south of the main star. That is also where Burnham's nebula extends the most.

2) A collision between two molecular clouds with a speed of the order of 10 km/s would undoubtedly produce a strong emission of shocked molecular hydrogen, another unusual characteristics of T Tauri. Evidence for bow shocks should be visible. We believe there is indeed such evidence on the H_2 emission images published in the literature (Van Langevelde *et al.* 1994, Quirrenbach and Zinnecker 1997). Dashed lines in Fig. 7 show C shaped features that could be produced by bow shocks. They are superposed to the map of Van Langevelde *et al*.. The arrows indicate the direction of the companion motion. At a smaller scale, there is also evidence for a similar

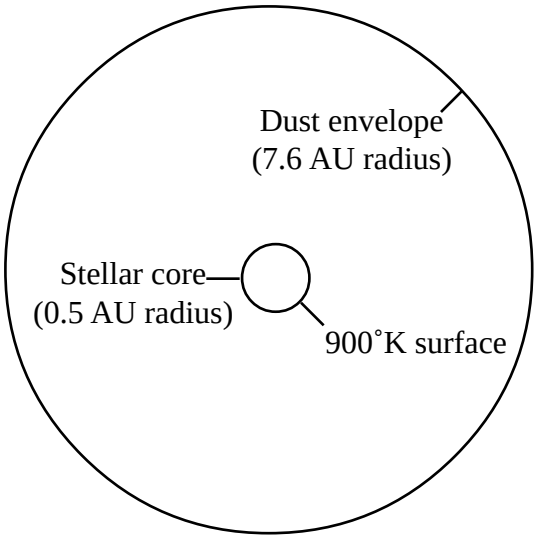

Fig. 8. Structure of T Tau South derived from the adaptive optics observations.

C-shape feature in the map of the HCO^+ millimetric emission published by Hogerheijde *et al*. (1997).

3) The arc seen in Fig. 1 could well be due to an accumulation of dust along a shock front surface east of T Tau North. Symmetrically, one should also expect an accumulation of dust in front of T Tau South but on the west side. This could explain the very bright tail. Heavy material might be pushed away and fall onto T Tauri North as observed, whereas lighter material might be blown away by the wind from T Tauri North and form the tail. Bubbles of heated gas expand as they slowly move away (Fig. 2).

4) Maps of the gas radial velocities around T Tauri have been obtained both in CO and ^{13}CO by Weintraub *et a*l. (1989) and in ^{13}CO by Momose *et al.* (1996). The CO maps show a blue shifted emission on the east side and a red shifted emission on the west side, which has been interpreted by Weintraub *et al*. (1989) as due to gas Keplerian motion from east to west in front of T Tauri. However, looking deeper in ^{13}CO, one sees both blue and red shifted motion on both sides. This has been interpreted by Momose *et al*. (1996) as produced by outflows along opposite parabolic cavities. Neither interpretation is fully satisfactory. On the other hand, these observations appear to be fully consistent with an east to west flow of gas both in front and behind T Tauri as one would expect from a collision with material coming from east.

5) The loss of the cocoon explains the companion lack of thermal emission longward of 3 μm, an emission normally expected from cold dust around a normal protostar (Ghez *et al*. 1991). Having lost its surrounding cocoon, the protostar becomes visible in the near infrared giving us a unique opportunity to observe its structure. Assuming blackbody radiation at ≈ 900˚K, the flux shown on top of Fig. 4 gives a stellar radius of 0.5 AU, smaller than the observed radius of 7.6 AU. We are therefore seeing light scattered by an envelope as described in Fig. 8. The radius of the envelope may correspond to the so-called centrifugal radius which describes the characteristic dimension of the collapsed configuration (Terebey et al. 1984).

6) Owing to conservation of the angular momentum, the core of a protostar is expected to rotate rapidly and produce a strong magnetic field. In addition, shocked gas probably accumulates west of T Tau South, close to T Tau North where it is subject to intense ionizing radiation from T Tau North. This may explain the enigmatic T Tauri radio source (Skinner and Brown 1994, Schwartz *et al*. 1986, Ray *et al*. 1997) and the unusually strong jet recently discovered by Reipurth et al. (1997).

Additional observations are needed to confirm that T Tau North and T Tau South are not gravitationally bound. If this is the case a more quantitative study of the above proposed scenario could be extremely fruitful.

Acknowledgements

We thank Alan Tokunaga for helping us process our 1993 data.

References

Akeson, R.L., Koerner, D.W. and Jensen, E.L.N. 1998. A circumstellar dust disk around T Tau N: sub-arcsecond imaging at λ = 3 mm, *Astrophys. J.* **505**, 358-362.

Beckwith, S.V.W., Gatley, I., Matthews, K., Neugebauer, G. 1978. Molecular hydrogen emission from T Tauri stars, *Astrophys. J*. **223**, L41-L43.

Bertout, C. 1983, T Tauri South: a protostar?, *Astron. Astrophys.* **126**, L1-L4.

Böhm, K.-H. and Solf, J. 1994. A sub-arcsecond-scale spectroscopic study of the complex mass outflows in the vicinity of T Tauri, *Astrophys. J*. **430**, 277-290.

Devaney, M.N., Thiébaut, E., Foy, R. et al. 1995. The Hα environment of T Tauri resolved by speckle interferometry, *Astron. Astrophys*. **300**, 181-188.

Dyck, H.M., Simon, Th. and Zuckerman, B. 1982. Discovery of an infrared companion to T Tauri, *Astrophys. J.* **255**, L103-L106.

Ghez, A.M., Neugebauer, G., Gorham, P. W. *et al*. 1991. Diffraction-limited infrared images of the binary star T Tauri, *Astron. J.* **102**, 2066-2072.

Ghez, A.M., Weinberger, A.J., Neugebauer, G., Matthews, K. and McCarthy Jr., D.W. 1995. Speckle imaging measurements of the relative tangential velocities of the components of T Tauri binary stars, *Astron. J*. **110**, 753-765.

Hanson, R. B., Jones, B. F. and Lin, D.N.C. 1983. The astrometric position of T Tauri and the nature of its companion, *Astrophys. J*. **270**, L27-L30.

Herbig, G.H. 1950. The spectrum of the nebulosity surrounding T Tauri, *Astrophys. J*. **111**, 11-14.

Herbst, W., Booth, J.F., Chugainov, P.F. *et al.* 1986. The rotation period and inclination angle of T Tauri, *Astrophys. J.* **310**, L71-L75.

Herbst, W., Beckwith, S.V.W., Glindemann, A. *et al*. 1996. A near-infrared spectral imaging study of T Tau, *Astron. J.* **111**, 2403-2414.

Herbst, T.M., Robberto, M. and Beckwith, S.V.W. 1997. *Astron. J*. **114**, 744-756.

Hogerheijde, M.R., van Langevelde, H. J., Mundy, L.G. *et al.* 1997. Subarcsecond imaging at 267 GHz of a young binary system: detection of a dust disk of radius less than 70 AU around T Tauri N, *Astrophys. J.* **490**, L99-L102.

Kobayashi, N., Nagata, T., Hodapp, K.-W. and Hora, J. 1994. Small outburst on the infrared companion of T Tauri finished, *Pub. Astr. Soc. Japan* **46**, L183-L186.

Leinert, Ch., Zinnecker, H., Weitzel, N. *et al*. 1993. A systematic search for young binaries in Taurus. *Astron. Astrophys*. **278**, 129-149.

Maihara, T. and Kataza, H. 1991. A study of the spatially-resolved T Tauri system, *Astron. Astrophys*. **249**, 392-396.

Momose, M. Ohashi, N., Kawabe, R. *et al.* 1996. The dispersing cloud core around T Tauri, *Astrophys. J.* **470**, 1001-1014.

Nakajima, T. and Golimowski, D.A. 1995. Coronagraphic imaging of pre-main-sequence stars: remnant envelopes of star formation seen in reflection, *Astron. J*. **109**, 1181-1198.

Quirrenbach, A. and Zinnecker, H. 1997. Molecular hydrogen towards T Tauri observed with adaptive optics, *The Messenger* **87**, 36-39.

Ray, T.P., Muxlow, T.W.B., Axon, D.J. et al. 1997. Large-scale magnetic fields in the outflow from the young stellar object T Tauri S, *Nature* **385**, 415-417.

Reipurth, B., Bally, J. and Devine, D. 1997. Giant Herbig-Haro flows. *Astron. J.* **114**, 2708-2735.

Roddier, C., Roddier, F., Northcott, M.J., Graves, J.E. and Jim, K. 1996. Adaptive optics imaging of GG Tau: optical detection of the circumbinary ring. *Astrophys. J*. **463**, 326-335.

Roddier, F., Roddier, C., Graves, J. E., Kim, K. and Northcott, M.J. 1995. Adaptive optics imaging at the CFHT, in Proc. of the *4th CFHT Users Meeting* (ed. M. Azzopardi, CFHT), 125-131.

Schwartz, P.R., Simon, Th. and Campbell, R.C. 1986. The T Tauri radio source. II. The winds of T Tauri. *Astrophys. J.* **303**, 233-238.

Skinner, S. L. and Brown, A. 1994. The enigmatic T Tauri radio source, *Astron. J*. **107**, 1461-1468.

Stapelfeldt, K.R., Burrows, C.J., Krist, J.E. *et al.* 1998. HST imaging of the circumstellar nebulosity of T Tauri, *Astrophys. J*. (in press).

Terebey, S., Shu, F.H. and Cassen, P. 1984. The collapse of slowly rotating isothermal clouds, *Astrophys. J.* **286**, 529-551.

Van Langevelde, H.J., Van Dishoek, E.F., Van der Werf, P.P. and Blake, A. 1994. The spatial distribution of excited H_2 in T Tau: a molecular outflow in a young binary system, *Astron. Astrophys.* **287**, L25-L28.

Weintraub, D. A., Masson, C. R. and Zuckerman, B. 1989. Measurements of Keplerian rotation of the gas in the circumbinary disk around T Tauri, *Astrophys. J*. **344**, 915-924.